New Phytologist

Characterization of the grapevine Shaker K+ channel VvK3.1 supports its function in massive potassium fluxes necessary for berry potassium loading and pulvinus-actuated leaf movements

Journal:	*New Phytologist*
Manuscript ID	Draft
Manuscript Type:	MS - Regular Manuscript
Date Submitted by the Author:	n/a
Complete List of Authors:	Nieves-Cordones, Manuel; Centro de Edafología y Biología Aplicada del Segura-CSIC, Nutricion Vegetal Andrianteranagna, Mamy; Institut Curie, Institut Curie Cuellar, Teresa; CIRAD, UMR1334 AGAP, PHIV-MRI Gibrat, Remy; BPMP, Univ Montpellier, CNRS, INRA, SupAgro, Montpellier, France, BPMP Boeglin, Martin; BPMP, Univ Montpellier, CNRS, INRA, SupAgro, Montpellier, France, BPMP Moreau, Bertrand; BPMP, Univ Montpellier, CNRS, INRA, SupAgro, Montpellier, France, BPMP Paris, Nadine; BPMP, Univ Montpellier, CNRS, INRA, SupAgro, Montpellier, France, BPMP Verdeil, Jean-Luc; CIRAD, PHIV Zimmermann, Sabine; CNRS Montpellier, Biochimie et Physiologie Moléculaire des Plantes, CNRS, INRA, Montpellier SupAgro, Univ. Montpellier, Gaillard, Isabelle; Univ Montpellier, CNRS, INRA, SupAgro, BPMP
Key Words:	berry K+ loading, paraheliotropic movements, phloem, pulvinus, Shaker K+ channel, VvK3.1 channel

Characterization of the grapevine Shaker K^+ channel VvK3.1 supports its function in massive potassium fluxes necessary for berry potassium loading and pulvinus-actuated leaf movements

M. Nieves-Cordones[1,3,°], M. Andrianteranagna[1,°], T. Cuéllar[2], R. Gibrat[1], M. Boeglin[1], B. Moreau[1], N. Paris[1], J.L. Verdeil[2], S.D. Zimmermann[1] and I. Gaillard[1*]

[1] BPMP, Univ Montpellier, CNRS, INRA, SupAgro, Montpellier, France
[2]CIRAD, UMR1334 AGAP, PHIV-MRI, 34398, Montpellier Cedex 5, France,
[3]Present address: Departamento de Nutrición Vegetal, CEBAS-CSIC, Campus de Espinardo, 30100 Murcia, Spain

Running title: Physiological role of the VvK3.1 channel in grapevine

*For correspondence (fax +33 4 67 52 57 37; e-mail isabelle.gaillard@inra.fr).
° MNC and MA have contributed equally to this work

Total word count: 6006

Word counts for: -Introduction: 859
-Materials and Methods: 1119
-Results: 1562
-Discussion: 2432
-Acknowledgements: 34

Number of figures: 8
Figures 1, 3 and 4 should be published in color
Number of Supplemental figures: 5
Figures S1, S2 and S5 should be published in color
Number of tables: 1

Summary (200 words)

- In grapevine, climate changes lead to increased berry potassium (K^+) contents that result in must with low acidity. Consequently, wines are becoming 'flat' to the taste, with poor organoleptic properties and low potential aging, resulting in significant economic loss. Precise investigation of the molecular determinants controlling berry K^+ accumulation during its development are only now emerging.
- Here, we report functional characterization by electrophysiology of a new grapevine Shaker-type K^+ channel, VvK3.1. The analysis of VvK3.1 expression patterns was performed by qPCR and *in situ* hybridization.
- We found that VvK3.1 belongs to the AKT2 channel phylogenetic branch and is a weakly rectifying channel mediating both inward and outward K^+ currents. We showed that *VvK3.1* is highly expressed in the phloem and in a unique structure located at the two ends of the petiole, identified as a pulvinus.
- From the onset of fruit ripening, all data support the role of the VvK3.1 channel in the massive K^+ fluxes from the phloem cell cytosol to the berry apoplasm during berry K^+ loading. Moreover, the high amount of *VvK3.1* transcripts detected in the pulvinus strongly suggests a role for this *Shaker* in the swelling and shrinking of motor cells involved in paraheliotropic leaf movements.

Keywords: berry K^+ loading, paraheliotropic movements, phloem, pulvinus, Shaker K^+ channel, VvK3.1 channel.

Introduction

Wines with a high standard of production are widely known for their characteristic flavors that reflect their environment (*e.g.* climate and soils) and their particular varieties. In the past, the climatic characteristics of different wine growing regions were properly taken into account to best adapt the vines to their environment. However, climate change is now affecting viticulture with high temperatures and soil water deficits that largely constrain grapevine productivity. Berry properties such as color, flavor, and aroma components are altered by these excessive solar radiation and severe drought conditions. Importantly, the impacts of climate change also result in unbalanced wines with excessively low acidity (Jones *et al.*, 2005; Kodur, 2011).

Grape acidity results from the ratio between free organic acids (*i.e.* malic and tartaric acids) and organic acids neutralized by potassium (K^+) ions. In grapevine berries, K^+ is involved as a major cellular counter-ion in the electrical neutralization of organic acids, in the control of pH, and in the fine-tuning of the acid-base balance of the flesh cells (Mpelasoka *et al.*, 2003; Kodur, 2011). However, the combined effects of climate change have a reducing effect on the free organic acid content, by increasing the consumption of malic acid as a respiratory substrate (Famiani *et al.*, 2016; Rienth *et al.*, 2016) and favoring K^+ accumulation during the ripening period (Kodur *et al.*, 2011; Duchêne *et al.*, 2014). Excess K^+ then interacts with tartaric acid to form K^+ bitartrate, which precipitates during the winemaking process. This results in musts with low acidity and consequently wines that are too sweet, with strong sensations of wood and alcohol (Mpelasoka *et al.*, 2003). Wine acidity, which normally allows flavor and aroma to develop during winemaking, is essential for the aging potential and also contributes to the red color of wine, through the degree of anthocyanin ionization (Mpelasoka *et al.,* 2003; Davies *et al.*, 2006).

The maintenance of berry quality can be achieved by controlling berry K^+ content at harvest. Nevertheless, this requires a better understanding of the molecular basis of K^+ accumulation throughout grape berry development, as well as improved identification of the different molecular actors involved in K^+ uptake and accumulation. In plants, K^+ accumulation is controlled by multigenic families that encode a broad spectrum of potassium transporters and channels as well as regulatory proteins (protein kinases, protein phosphatases, *etc.*) (Dreyer and Uozumi, 2011; Sharma *et al.*, 2013; Ronzier *et al.*, 2014; Véry *et al.*, 2014; Lefoulon *et al.*, 2016).

Among the different K^+ transport systems that have been identified and characterized in grapevine (Pratelli *et al.*, 2002; Davies *et al.*, 2006; Cuéllar *et al.*, 2010, 2013), only two currently appear to be involved in the loading of this cation into grape berries during the ripening stage (Hanana *et al.*, 2007; Cuéllar *et al.*, 2013). The first transport system, VvK1.2 (Cuéllar *et al.*, 2013), is a voltage-gated inwardly rectifying K^+-selective channel that belongs to the K^+ Shaker channel family. *VvK1.2* is specifically expressed in the berry, strongly emerging in the plasma membrane of the flesh cells (mesocarp) and the perivascular cells at veraison (the onset of ripening). Its expression level then continuously increases during berry ripening and can be strongly increased further by mild drought stress. The expression pattern and transcriptional regulation of VvK1.2 both indicate that this channel likely plays a major role in K^+ uptake in flesh cells of ripening berries (Cuéllar *et al.*, 2013). The second transport system, VvNHX1, is a vacuolar cation$^+$/H^+ antiporter belonging to the NHX type of transporter families (Hanana *et al.*, 2007). VvNHX1 mediates Na^+/H^+ and K^+/H^+ coupled exchange, with a higher affinity for K^+ than Na^+. Moreover, VvNHX1 expression is strongly increased starting from veraison and during berry maturation, indicating that this transporter may be responsible for vacuolar accumulation of K^+ at the inception of ripening, driving the uptake of water that generates vacuolar expansion (Hanana *et al.*, 2007).

Here, we report the characterization of the grape Shaker K^+ channel VvK3.1. In plants, Shaker genes are known to encode highly K^+-selective channels that are strongly voltage-regulated. These channels are active at the plasma membrane and provide major pathways for bulk K^+ uptake or secretion in various tissues and cell types (Sharma *et al.*, 2013; Véry *et al*., 2014). We demonstrate that VvK3.1 is a weak inwardly rectifying K^+ channel that is only slightly activated by CBL-interacting Ser/Thr protein kinase (CIPK)/calcineurin B-like Ca^{2+} sensor (CBL) complexes. This channel is highly expressed in all grapevine organs, with expression restricted to the phloem and phloem parenchyma. We found that *VvK3.1* expression in the phloem continuously increases during berry ripening, suggesting a major role for this Shaker channel in the unloading of K^+ from phloem during grape maturation. This is a major concern for grapevines, as the fruit is energetically limited due to stomata disappearance after veraison. Unexpectedly, in addition to the phloem, VvK3.1 is expressed in particular structures localized at the joints of the petiole that display the histological features of a pulvinus, *i.e.* a motor organ known to be involved in plant leaf movements. Finally, the roles played by the VvK3.1 channel both in K^+ loading into berry tissues and in grapevine leaf movements are discussed.

Materials and Methods

Plant materials

Four-year-old grapevines (*Vitis vinifera* cv. Cabernet Sauvignon) were grown in field conditions within 70-l containers. The controlled watering process used to obtain plants with different water statuses has been described previously (Cuéllar *et al*., 2010, 2013). Drought conditions were produced by subjecting plants to a reduced irrigation program over a period of 2 weeks, prior to measuring the leaf water potential (ψ) for at least 2 days before tissue collection (Cuéllar et al., 2010). The ψ value ranged from -0.7 to -0.6 MPa in drought-treated plants, whereas ψ remained close to -0.2MPa at dawn for control plants that were not subjected to drought stress. All samples were collected at fruit set period with the exception of berry samples, which were harvested at various stages of grape development. Roots and leaves were collected from 2-month-old rooted canes planted in perlite (Cuéllar *et al*., 2010). Samples were immediately frozen in liquid nitrogen before being used in the different experiments. For *in situ* hybridization and histology experiments, fresh organs were collected only in the control condition and were directly embedded in paraffin.

Isolation of cDNAs encoding VvK3.1, VvCIPK and VvCBL proteins

First strand cDNAs from grapevine were synthesized from total RNA prepared from post-veraison berries using SuperScript III RT polymerase (Invitrogen 18080-051). *VvK3.1* was cloned before the grape genome sequence was made available (Jaillon *et al*., 2007; Velasco *et al*., 2007) through a three-step strategy. First, two overlapping EST (expressed sequence tag) sequences (CF518215 and CF519070) corresponding to the 3' region of *VvK3.1* cDNA were identified in the *Vitis vinifera* cv. Cabernet Sauvignon EST library (LIBEST_014375). These were used to design the cf-5' and cf-3' specific primers (Table S1), which amplify a 963 bp fragment. Next, the primers PTK25'-1 and PTK25'-3 were designed based on alignments of group 3 plant Shaker channels identified in different plant species (*Arabidopsis thaliana*, *Solanum lycopersicum*, *Solanum tuberosum, Hordeum vulgare*;
http://biowed.pasteur.fr/seqanal/interfaces/clustalw.html). A *VvK3.1* cDNA fragment encoding the conserved domains of the channel's hydrophobic core and its C-terminal domain was amplified through two successive PCR runs with PTK25-1/cf-3' and PTK25'-

3/cf3'-2. Finally, 5' RACE was performed to obtain the 5' end of *VvK3.1* cDNA, using the primers AS5, AS6 and AS8.

The corresponding full-length clone (GenBank/EMBL XM_002268888.3) was generated by nested PCR using primers flanking the 5' and 3' ends of the coding sequence (first step: full5'kt2f1/full3'KT2R1, second step: full5'KT2atgF2/fullKT2withtaaR2) before subcloning into the PCI vector and verification by sequencing of both strands.

VvCIPK03 (Gene ID: 100241657) and *VvCIPK02/05* (Gene ID: 100261839), the closest relatives of *A. thaliana* CIPK6, were previously cloned (Cuéllar *et al.*, 2013). *VvCBL04* (Gene ID: 100246874), the closest relative of *A. thaliana CBL4*, was cloned through nested PCR using VvCBL04F1/VvCBL04R1 and VvCBL04F2/VvCBL04R2 from post-veraison berries. Sequencing of the PCR products confirmed that it corresponds to the expected cDNA.

Localization of *VvK3.1* expression by mRNA *in situ* hybridization

In situ hybridization experiments were performed as described by Cuéllar *et al.* (2010). Briefly, *VvK3.1* RNA probes were synthesized using the *VvK3.1*-specific primers K3.1-124-F/K3.1-124-R (Table S1). An 18S ribosomal probe was used as the control. Sense and antisense probes were labelled with UTP-digoxigenin during the transcription step. Explants from roots, leaves, petioles and berries at different developmental stages were fixed in 4% paraformaldehyde and embedded in paraffin (Cuéllar *et al.*, 2010). Samples were cut into 8-µm sections and hybridized overnight before incubation for 1 h at 37°C in the presence of anti-DIG antibody conjugated with alkaline phosphatase (1/500 dilution; Roche, http://www.roche.com). Hybridization signals were detected using either the VectorBlue KIT III (Vector Laboratories, http://www.vectorlabs.com; positive signal is blue) or the BCIP/NBT substrate system (Dako; positive signal is purple). Slides were observed with a DM600 microscope (Qimaging, http://www.qimaging.com) and images were taken with a Qimaging Retiga2000R camera**.**

Histological staining of petiole cross sections

Petioles were fixed for 24 h in a solution containing 1% glutaraldehyde, 2% paraformaldehyde and 1% caffeine in 0.2 mM phosphate buffer at pH 7.2. Subsequently, the samples were dehydrated through an ethanol series, embedded in Technovit 7100 resin

(Heraeus Kulzer), and cut into 3-µm semi-thin sections. These sections were stained with periodic acid-Schiff, which stains polysaccharides (*i.e.* walls and starch) in red, and naphthol blue-black, which stains both soluble and insoluble proteins in blue. Sections were observed by conventional light microscopy using a DM6000 Leica microscope and photographed.

Total RNA extraction and real-time quantitative RT-PCR analysis

Total RNA extractions from various tissues (leaves, stems, petioles, tendrils and berries at different developmental stages) were performed using the Plant RNeasy extraction kit (QIAGEN, Germany), using the modifications described in Cuéllar *et al*. (2010). First-strand cDNAs were synthesized with SuperScript III reverse transcriptase (Invitrogen) and used as template for quantitative RT-PCR experiments, as previously described (Cuéllar *et al*., 2010, 2013). Oligonucleotides were designed using Primer3 (http://frodo.wi.mit.edu/). Primer pair sequences that are specific to *VvK3.1* (K3.1-124-F/K3.1-124-R) and elongation factor 1-alpha (EF1-F/EF1-R; Cuéllar *et al.*, 2010) are provided in Table S1.

Functional characterization of VvK3.1

Oocyte handling and voltage clamp experiments were performed as previously described (Cuéllar *et al*., 2010, 2013). *VvK3.1* cRNAs (6 ng) were injected using a microinjector (Nanoliter 2000, WPI, http://www.wpi-europe.com/fr/) into *Xenopus laevis* oocytes. For co-expression experiments with VvCIPK03 or 02/05 and VvCBL04, the same amount of *CIPK/CBL* (1:1) cRNA was injected. Control oocytes were injected with water (23 nl) or *CIPK/CBL* cRNA. Injected oocytes were maintained at 19°C in a standard solution (ND96; pH 7.4) containing 96 mM NaCl, 2 mM KCl, 1 mM MgCl, 1.8 mM $CaCl_2$, 5 mM HEPES, and 2.5 mM sodium pyruvate, supplemented with gentamycin sulfate (50 µg ml^{-1}). Membrane currents were measured 3-5 days after injection with a two-microelectrode voltage clamp amplifier (GeneClamp 500B; Axon Instruments, http://www.moleculardevices.com) and a Digidata 1322A interface (Axon Instruments). Pipettes were filled with solutions of 3 M KCl containing 100 (K100), 50 (K50) or 10 mM (K10) potassium gluconate, supplemented respectively with 0, 50 or 90 mM sodium gluconate in 1 mM $CaCl_2$, 2 mM $MgCl_2$, and 10 mM HEPES (pH 6.5 or 7.5) or 10 mM MES (pH 5.5). Inhibition by Cs^+ or Ba^{2+} was assayed by addition of 10 mM CsCl or 30 mM BaCl to the K100 solution at pH 6.5. Voltage clamp protocols were applied with 1.4 s voltage pulses from +70 to -155 mV (or -170 mV), in -15 mV steps, followed by a 250-ms

voltage step to -40 mV at a holding potential of 0 mV. Normalized current–voltage (I–V) curves were obtained by plotting steady-state currents at the end of activating voltage pulses against corresponding applied membrane potentials, setting the current value at -140 mV in K100 at pH 6.5 to -1 for each oocyte. Voltage-pulse protocols, data acquisition and analysis were performed using the pClamp 10 program suite (Axon Instruments).

Results

Identification of the grapevine K^+ channel *VvK3.1*

Alignments of pore-forming and cyclic nucleotide-binding domains of K^+ channels cloned in plants were used to design adequate primers for identifying grapevine homologs of *A. thaliana* Shaker K^+ channels. A 2,526 bp cDNA was obtained from the total RNA of post-veraison *Vitis vinifera* (cv. Cabernet Sauvignon) berries, using a combination of reverse transcription (RT)-PCR amplifications and 5' RACE extension. The deduced amino acid polypeptide contains 841 residues and shares sequence homology with other plant Shaker channels. Phylogenetic analysis revealed that this grape *Shaker*, subsequently named VvK3.1, is related to AKT2 and belongs to group III of the plant Shaker K^+ family (Fig. 1a). The corresponding polypeptide displays 68% amino acid sequence identity (ASI) throughout the entire protein length with its *A. thaliana* counterpart, AKT2 (Lacombe *et al.*, 2000). Of particular note is that group III is composed of a single member in both the *A. thaliana* and grapevine Shaker families. Sequence analysis of the VvK3.1 polypeptide identified the typical structural regions of Shaker subunits (Fig. 1b), with a short N-terminal cytosolic domain followed by 6 transmembrane segments. This includes a well-defined pore region between the fifth and the sixth transmembrane domain which contains the potassium-selective signature sequence "TXXTXGYGD" (Dreyer *et al.*, 1998). The large cytosolic C-terminal part begins just after the end of the sixth transmembrane domain (S6) and successively contains a C-linker domain, a cyclic nucleotide-binding domain (CNBD), an ankyrin domain, and a K_{HA} domain (Ehrhardt *et al.*, 1997; Sharma *et al.*, 2013; Nieves-Cordones *et al.*, 2014; Véry *et al.*, 2014).

The Shaker K^+ channel gene *VvK3.1* is expressed in all tested grapevine organs

To evaluate the expression pattern of the *VvK3.1* gene in various grapevine organs, real-time PCR was performed on total RNA extracted from leaves, stems, petioles, tendrils,

roots and berries at different stages of development. High *VvK3.1* transcript levels were detected in all analyzed samples (Fig. 2a). This result is in agreement with the previous observation that group III Shaker subunits (AKT2 branch) display the broadest expression spectrum (Lacombe *et al.*, 2000; Ache *et al.*, 2001; Langer *et al.*, 2002). *VvK3.1* expression in grape berries increased during grape development, reaching a maximal amount in ripe berries (Fig. 2b).

To check the *VvK3.1* expression profile at different developmental stages, *in situ* hybridization analyses were conducted in flowers, as well as in berries at the fruit set and ripening (post-veraison) stages (Fig. 3). In flowers, *VvK3.1* transcripts were detected in the phloem (Fig. 3a6). An intense signal was also observed in the inner part of the ovule, named the nucellus, where the embryo sac develops (Fig. 3a4). *VvK3.1* expression was also detected to a lesser extent in the epidermis of ovarian locules and at the base of stigmas (Fig. 3a3-a6). During the fruit set stage in berries, *VvK3.1* expression was mainly detected in the phloem and in the endosperm, a storage tissue that is derived from double fertilization (Fig. 3b2-b4). During the ripening stage (post-veraison period), *VvK3.1* expression was strongly restricted to the phloem and perivascular cells (Fig. 3c3-c5). High levels of *VvK3.1* transcripts were exclusively detected in the phloem of leaves (Fig. S1) and roots (Fig. S2).

Interestingly, aside from its expression in the phloem, *VvK3.1* was identified in a structure located at both extremities of the petiole (Fig. 4a1-2, white arrows, and c3-6). When drought stress was applied by stopping plant irrigation, these particular zones of the petiole became curved, bringing the leaf parallel to the stem (Fig. 4a1-2). Histological examination of this part of the petiole (Fig. 4b1-3) revealed an asymmetrical organization with specific cell layers organized around the vascular systems at the abaxial face of the petiole (Fig. 4a4, abs). This organization is consistent with a pulvinus structure, as shown under higher magnification (Fig. 4b). In this zone we observed the presence of two different cell types: small cells with large pectin walls, in the outer cell layers (Fig. 4b2-3, red staining); and thin-walled large parenchyma cells containing a large vacuole, in the innermost cell layers (Fig. 4b-c). It is important to note that *VvK3.1* expression is detected in both of these cell layers (Fig. 4c5). In plants, the pulvini are involved in leaf movements that occur in response to a variety of endogenous and exogenous stimuli (Moran, 2007), although so far this structure has not been described in grapevine.

Effect of drought stress on *VvK3.1* expression

The response of grapevine to water stress is highly dependent on the variety and the rootstock, although a limited water stress is generally considered to be beneficial for berry quality. It has been demonstrated, from the start of the veraison stage, that grapevine is relatively tolerant to water deficit. Furthermore, regulated irrigation has been advantageously used to inhibit vine growth without any reduction in berry yield (Kennedy *et al*., 2000; Esteban *et al*., 2001). Here, the effects of moderate drought stress (-0.7 to -0.6 MPa for at least 2 days before tissue harvesting) were reproduced in field conditions, as described above. Berries were sampled after flowering (AF) at three stages of development: post-fruit set stage (day 25 AF), veraison (day 60 AF), and during ripening (day 75 AF). *VvK3.1* expression in berries was then investigated by real-time quantitative PCR (qPCR), and a slight increase in VvK3.1 transcript levels was observed upon drought stress (Fig. 5a), particularly in the early stages. Nevertheless, this induction of *VvK3.1* transcript in response to drought stress was far less considerable than the quantity previously observed for *VvK1.2* (Cuéllar *et al.*, 2013).

VvK3.1 transcript accumulation was also investigated by qPCR in leaves and roots harvested from water-stressed or control rooted canes. Drought stress, induced by stopping irrigation, was found to have different effects on *VvK3.1* transcript levels in roots and leaves. Specifically, drought stress increased *VvK3.1* transcript accumulation in leaves (Fig. 5b) but had no effect on the level of *VvK3.1* in roots (Fig. 5c). In leaves, a significant (threefold) up-regulation in *VvK3.1* was observed in response to water stress.

VvK3.1 behaves as a weak K^+ inward rectifier channel in *Xenopus* oocytes

Functional properties of the grapevine channel VvK3.1 were investigated in *Xenopus laevis* oocytes. Instantaneous and time-dependent currents (Fig. 6a) were reminiscent of those observed with the *A. thaliana* Shaker channel AKT2 previously characterized as a weak K^+ inward rectifier channel (Philippar *et al.*, 1999; Lacombe *et al.*, 2000; Ache *et al.*, 2001; Langer *et al.*, 2002). The observed currents were dependent on external potassium concentrations and exhibited smaller amplitudes at reduced external K^+ concentrations (Fig. 6b). Reversal potentials were found to shift towards more hyperpolarized potentials in response to decreasing K^+ concentrations (Fig. S3a). VvK3.1 was inhibited in a voltage-dependent manner by Cs^+ (Fig. 6c), with an increase in channel blocking at more negative potentials as previously described for AKT2 (Lacombe *et al*., 2000). Addition of 30 mM Ba^{2+} also provoked a strong inhibition of currents (Fig. S3b), reminiscent of the complete AKT2 blocking by Ba^{2+} (Marten *et al*., 1999).

Acidification of the external solution reduced VvK3.1 current amplitudes (Fig. 7a), as shown similarly for *A. thaliana* AKT2 channel activity (Lacombe *et al*., 2000), and in contrast to the behavior of inward rectifiers such as VvK1.2 (Cuéllar *et al*., 2013). Indeed, VvK3.1 activity was stimulated by an increase in external pH, suggesting an interference of protons with the channel permeation. Upon external acidification, the proportions of instantaneous as well as time-dependent currents were modified. For VvK3.1, inhibition of the time-dependent component was slightly stronger than that of the instantaneous current (Fig. 7b). This should result in a reduced inward rectification capacity of its residual current, whereas the opposite was found for AKT2 (Lacombe *et al.,* 2000).

Another level of Shaker K^+ channel activity regulation is based on CIPK-CBL interactions. Indeed, the *A. thaliana* Shaker channel AKT2 was previously shown to be regulated by the CIPK6/CBL4 complex (calcineurin B-like (CBL)-interacting protein kinase 6 (CIPK) and Ca^{2+}-sensing CBL 4 partners) (Held *et al*., 2011). Since the mechanisms of K^+ channel regulation involving CIPK–CBL complexes are conserved between *A. thaliana* and grapevine for other Shaker-type channels (Cuéllar *et al*., 2010, 2013), we also evaluated this regulation for VvK3.1. Thus, cDNAs from *VvCIPK03*, *VvCIPK02/05* and *VvCBL04*, which are the closest grapevine relatives of *A. thaliana AtCIPK6* and *AtCBL4* (Fig. S4), were cloned from post-veraison berries to assess whether this regulatory pathway is conserved in grapevine. When expressed without the channel, the VvCIPK03/VvCBL04 and VvCIPK02/05/VvCBL04 complexes did not elicit any significant currents in oocytes in comparison to water-injected oocytes (Fig. 8a, top). Conversely, even though the VvK3.1 channel was able to mediate K^+ currents when expressed alone (Fig. 8a, middle), co-expression with these two CIPK/CBL partners led to an increase in the current magnitude (Fig. 8a, bottom). Indeed, co-expression of VvK3.1 together with VvCIPK03/CBL04 significantly increased the K^+ current by about 60% at -140 mV, in comparison to the current recorded when the VvK3.1 channel was expressed alone in oocytes (Fig. 8b). The other tested CIPK-CBL complex, VvCIPK02/05/VvCBL04, provoked a weaker increase in K^+ current, by about 20% at -140 mV (Fig. 8b). Finally, it is worth noting that the relative proportions of the instantaneous and time-dependent components of the VvK3.1 currents were not altered by these two CIPK/CBL complexes (Fig. 8C). Similarly, when the AKT2 channel is co-expressed with AtCIPK3-AtCBL4 complex, no significant change in the proportion of the two current components is observed (Held *et al*., 2011).

Discussion

The grapevine VvK3.1 and *A. thaliana* AKT2 channels share functional properties

In grapevine, VvK3.1 is the only subunit belonging to the third group of Shaker channels representing a subfamily of weak rectifiers. Similarly, this group contains a single subunit in *A. thaliana*, named AKT2. With 68% amino acid sequence identity, VvK3.1 is the closest relative of AKT2 in grapevine (Fig. 1). The *Arabidopsis* AKT2 channel is known to dominate the phloem K^+ conductance in both sieve and companion cells, where it has a major role in phloem K^+ loading and unloading (Marten *et al.*, 1999; Deeken *et al.*, 2000, 2002; Lacombe *et al.*, 2000; Ache *et al.*, 2001; Philippar *et al.*, 2003; Ivashikina *et al.*, 2005; Hafke *et al.*, 2007). When expressed in *X. laevis* oocytes, the AKT2 channel forms a weakly rectifying channel, thereby giving rise to two current components with different gating modes (Marten *et al.*, 1999; Lacombe *et al.*, 2000; Dreyer *et al.*, 2001; Michard *et al.*, 2005a). This unique feature allows AKT2 to mediate inward as well as outward K^+ currents. As shown in Fig. 8, the VvK3.1 channel can also combine two gating modes: a time-dependent voltage-activated current, and an instantaneous ohmic current, like AKT2. Although it has been described that AKT2 can switch between these gating modes *via* post-translational regulation (Michard *et al.*, 2005a), the underlying mechanisms are still not fully understood (Sandmann *et al.*, 2011).Two serine residues (S210 and S329), with one located in the S4–S5 linker and the other in the C-linker, have been identified as phosphorylation targets (Dreyer *et al.*, 2001; Michard *et al.*, 2005a, 2005b). Moreover, the lysine (K197) located within the voltage sensor region enables AKT2 to sense its phosphorylation status and to change between the two modes (Michard *et al.*, 2005b; Sandmann *et al.*, 2011). Interestingly, these two serines and this lysine are present in the corresponding position in the VvK3.1 sequence, strongly indicating that VvK3.1 behaves similar to AKT2.

Moreover, in oocytes, the AKT2-like channels are inhibited upon external acidification (Marten *et al.*, 1999; Philippar *et al.*, 1999; Lacombe *et al.*, 2000; Langer *et al.*, 2002). Our results demonstrate that the VvK3.1 channel displays a similar pH sensitivity, with one minor difference: the relative proportions of the instantaneous and time-dependent currents are differently disturbed as compared to AKT2 (Fig. 7). Indeed, external acidification results in an increased inward rectification of the AKT2 residual current (Lacombe *et al.*, 2000), whereas under the same conditions the instantaneous component prevails in the

VvK3.1 residual currents.

In addition, several reports have identified associations between AKT2 and different putative partners (Chérel *et al.*, 2002; Held *et al.*, 2011; Sklodowski *et al.*, 2017). For example, the association of AKT2 with the AtCIPK6/AtCBL4 complex gives rise to an increase in macroscopic AKT2 currents, by enhancing the targeting of AKT2 to the plasma membrane (Held *et al.*, 2011). Since VvK3.1 appears to be closely related to AKT2, we assumed that a homologous regulatory network could control its activity at the cell membrane. In *X. laevis* oocytes, co-expression of VvCBL04 with VvCIPK03 or VvCIPK02/05, the closest relatives respectively of AtCBL4 and AtCIPK6 (Fig. S4) (Cuéllar *et al.,* 2013), produced an increase in the VvK3.1 current. This increase displayed a higher magnitude in the VvCIPK03-VvCBL04 pair (Fig. 8). Moreover, no significant effect on the relative proportions of the instantaneous and time-dependent currents was observed (Fig. 8c), similar to previous observations with AKT2 (Held *et al.,* 2011). Overall, the functional properties of VvK3.1 and AKT2 indicate that these two channels have very similar behaviors, providing additional support to the phylogenetic relationship between them and the group III plant Shaker K^+ channels. More generally, our results, together with those described earlier for VvK1.1 and VvK1.2 (Cuéllar *et al.*, 2010, 2013), reinforce the observation that the mechanisms of K^+ channel regulation by CIPK–CBL complexes are conserved between *A. thaliana* and grapevine.

Role of the VvK3.1 channel in berry K^+ loading

Berry development consists of two successive growth periods. The first period comprises a rapid cell division phase followed by marked cell enlargement. This period is characterized by the synthesis and vacuolar storage of tartaric and malic acids. The second period commences with veraison, at the onset of ripening. At veraison, the berry starts to change color and soften, as it becomes a strong sink for water, K^+, sugar and solute imports (Davies *et al.*, 2006; Conde *et al.*, 2007). At this stage, berry loading is dependent on phloem sap flux, since the xylem has become non-functional (Keller *et al.*, 2006; Chatelet *et al.*, 2008a, 2008b; Choat *et al.*, 2009; Knipfer *et al.*, 2015). Moreover, K^+ transport in the berry switches from the symplasmic to the apoplasmic mode (Zhang *et al.*, 2006), meaning that unloaded solutes must cross plasma membranes at least twice before accumulating within the berry mesocarp. Previous research has posited that berry loading *via* an apoplasmic mode should reduce the transport of apoplasmic solutes out of the

438 berries (Findlay *et al.*, 1987; Mpelasoka *et al.*, 2003) and improve the control of efficient
439 long-distance phloem transport from source leaves to ripening berries (Zhang *et al.*, 2006).
440 Starting at veraison, the VvK3.1 channel is highly expressed in the berry phloem (Figs. 2
441 and 3) and becomes the obvious candidate for loading K^+ into the berry. The unique
442 functional characteristics of the VvK3.1 channel are indeed suited for this. In this scenario,
443 the VvK3.1 channel would be switched from an inward-rectifying to a non-rectifying mode,
444 so as to enable massive K^+ efflux, *i.e.* K^+ secretion into the berry mesocarp apoplasm.
445 Taking into account previous studies on AKT2 functioning (Marten *et al.*, 1999; Lacombe
446 *et al.*, 2000; Dreyer *et al.*, 2001; Michard *et al.*, 2005a, 2005b) and the fact that the AKT2
447 and VvK3.1 channels have very similar functional behaviors, VvK3.1 should be locked in
448 the open state in its phosphorylated form across the entire physiological voltage range.
449 Therefore, this channel may drive the K^+ efflux that allows K^+ ions to move down their
450 transmembrane concentration gradient (100 mM in the phloem cell cytoplasm and 1 mM in
451 the apoplasm; Ache *et al.*, 2001; Wada *et al.*, 2008).
452 It is known that K^+ gradients play a major role in driving sugar, amino acid and water
453 transport across plant cell membranes during phloem unloading (Ache *et al.*, 2001;
454 Philippar *et al.*, 2003). However, the remarkable increase in solute import in berries at
455 veraison signifies a challenge in terms of transport energization. Electrochemical gradients
456 dependent on the H^+-ATPase activity may be reduced in berries since, from the start of
457 veraison, the stomata are no longer functional, photosynthesis has stopped, and ATP
458 synthesis mostly depends on cellular respiration with malic acid as the substrate (Kanellis
459 and Roubelakis-Angelakis, 1993). Under such circumstances, the recent concept of a K^+
460 battery for transmembrane transport processes seems appropriate, since it provides
461 additional energy stored in the K^+ gradient between the phloem cytosol and the berry
462 apoplasm (Gajdanowicz *et al.*, 2011; Sandmann *et al.*, 2011; Dreyer *et al.*, 2017). The K^+
463 battery also explains how an open AKT2-like channel, like VvK3.1, can drive K^+ ions
464 from the cytosol to the apoplasm as well as reinforce the transmembrane electrical gradient
465 by hyperpolarizing the plasma membrane potential. This electrical gradient can
466 compensate for the reduced pH gradient present under energy limitation. Furthermore, it
467 can be used to retrieve sucrose from the apoplasm and to maintain sucrose levels in the
468 phloem vessels until reaching the different sites of unloading.
469 In grapevine, sucrose is used for long-distance transport in the phloem from source leaves
470 to grape berries, and sugar loading into berries is performed from veraison onward and

during the ripening period (Kuhn and Grof, 2010; Lecourieux *et al.*, 2014). Anatomical sections of grape berries reveal a large network of vascular bundles with a central capillary bundle and many major and minor peripheral capillary bundles that irrigate the berry (Zhang *et al.*, 2006). This observation strongly suggests that sucrose retrieval could be performed over the entire length of the grape berry's vascular bundle (from the different sites of phloem unloading), in order to distribute the large amount of sucrose to all parts of the berry mesocarp apoplasm.

The main advantage of this K^+ battery mechanism is that it does not require ATP consumption (Dreyer *et al.*, 2017). Thus, it is tempting to speculate that the non-rectifying mode of VvK3.1 contributes to K^+ secretion into the grape berry apoplasm, in addition to switching on the K^+ battery to allow sucrose retrieval in energy-limited conditions. At this stage, the inwardly rectifying VvK1.2 channel (Cuéllar *et al.*, 2013) that is highly expressed in flesh cells and perivascular cells surrounding the vascular bundles would then contribute to the berry loading mechanisms. In particular, this Shaker channel is strongly activated by interacting with specific VvCIPK/VvCBL pairs. This can allow rapid absorption of K^+ by perivascular cells and then by flesh cells to keep the apoplasmic K^+ concentration at low levels, despite the efflux from the phloem stream. Indeed, since the transmembrane gradient of K^+ can be maintained between phloem cells and the berry apoplast, the phloem stream flux towards the sink may be stimulated and employment of the K^+ battery process for sucrose retrieval may persist over a long period of time. This latter process should also allow saving ATP, which in grape berry is locally produced by cell respiration, for other transport mechanisms driven by ATP-consuming H^+-ATPase.

VvK3.1 and K^+ transport in the grapevine pulvinus

In addition to the phloem, *VvK3.1* is also strongly expressed in a second tissue located at the two ends of the petiole (Fig. 4). The careful histological examination of this zone (Fig. 4. a1-2) enabled us to identify this as a specialized motor organ known as the pulvinus. Nastic, paraheliotropic and diaheliotropic movements are mediated by this organ, allowing it to play a key role in leaf movements (Pastenes *et al.*, 2004). Because grapevine is a major crop in both warm and drought-prone areas, this plant has the ability to perform solar tracking in order to reduce leaf temperature and transpirational water loss, and protect its photosynthetic activity. In this context, several studies on the impacts of excess light on the photosynthesis rate in grapevine leaves have been conducted (During, 1988; Iandolino *et al.*, 2013; Keller, 2015). High irradiance induces photodamage to photosystem II (PSII)

in leaves (Adir *et al.*, 2003; Pastenes *et al.*, 2004; Takahashi *et al.*, 2009) and leads to photoinhibition, which can limit plant photosynthesis activity, growth and productivity. Several mechanisms have been identified to protect or repair PSII under conditions of excess light energy (Müller *et al.*, 2001; Takahashi *et al.*, 2007, 2009; Huang *et al.*, 2012). Among them, leaf movements have been observed in several plant species in response to direct sunlight (Takahashi and Badger, 2011). In a light-avoiding movement known as paraheliotropism, the grapevine leaves orient at an angle parallel to the sun's rays (Iandolino *et al.*, 2013; Keller, 2015). This movement helps to prevent photodamage of PSII and minimizes photoinhibition (Pastenes *et al.*, 2005; Takahashi *et al.*, 2009). Paraheliotropic movements are also observed when environmental conditions change, *e.g.* when exposed to excess light, high temperatures, or drought stress (During, 1988; Pastenes *et al.*, 2005; Iandolino *et al.*, 2013).

These grapevine leaf movements are governed *via* common plant mechanisms based on differentially changing cell turgor within the pulvinus. Substantial information about pulvinus structure and function has been gained by studying the nyctinastic leguminous tree *Samanea saman* (Satter *et al.*, 1981; Gorton, 1987a, 1987b; Yu *et al.*, 2001, 2006). In this species, two groups of specialized motor cells arranged in two opposite zones can be distinguished in the pulvinus: the flexor cell, located in the adaxial side; and the extensor cell, located in the abaxial side (Uehlein and Kaldenhoff, 2008). Similar to the guard cells, solute content and ion composition (which are mainly dependent on potassium) induce osmotic water fluxes in the motor cells, allowing them to change their volume and shape according to turgor changes. Accordingly, uptake of K^+ can lift the leaves through swelling of the abaxial extensor cells, concomitant with shrinking of the adaxial flexor cells (Fig. 4a). Upon redistribution of potassium ions, the opposite effect takes place: the extensor cells shrink and the flexor cells swell, lowering the position of the leaves (Fig. 4b) (Gorton, 1987a and b; Satter *et al.*, 1974). Moreover, our *in situ* hybridization experiments detected an intense expression of *VvK3.1* in this structure, which was restricted to the abaxial side of the pulvinus, where the extensor cells are usually found (Fig. 4c3).

Taking into account the unique functional features of VvK3.1, we propose that this channel mediates both inward and outward K^+ currents to allow for the influx or efflux of potassium involved in either the swelling or shrinking of extensor cells. The activity of VvK3.1-like channels has already been recorded in *Samanea saman* motor cells, with results that support our hypothesis (Moshelion *et al.*, 2002; Yu *et al.*, 2006). Interestingly, pH values recorded in the *Samanea saman* extensor apoplast have been observed to range

539 from 6.5 to 7.2 (Lee and Satter, 1989), which would be compatible with a significant
540 VvK3.1 activity in extensor cells. Since VvK3.1 is only expressed in extensor cells, two
541 alternative hypotheses may be considered for the mechanism that takes place in flexor
542 cells. The first one is that the elasticity of pectin walls in the parenchyma cells of the flexor
543 tissue is sufficient to facilitate and accommodate leaf movements. The second hypothesis
544 speculates that there are other transport systems involved in K^+ conductance in grapevine
545 flexor cells (Yu *et al.*, 2001; Moshelion *et al.*, 2002).
546 Here, we have provided evidence that the VvK3.1 channel, in addition to its role in
547 grapevine pulvinus functioning, may play a key role in berry loading during grape berry
548 ripening by controlling phloem K^+ transport. In grape berries, veraison occurs at a time of
549 profound developmental changes. The shift from the symplasmic to the apoplasmic mode
550 of phloem unloading modifies the translocation pathways. The VvK3.1 and VvK1.2
551 (Cuéllar *et al.*, 2013) channels are both expressed in perivascular cells (Fig. S5), and are
552 likely involved in the reorganization of the K^+ transport mechanisms that take place during
553 the loading of ripening berries. Moreover, the expression of these two channels is
554 upregulated upon drought stress exposure, suggesting a compensatory measure to control
555 K^+ transport, thereby preventing the decrease of water availability. Our results strongly
556 indicate that a better understanding of the mechanisms regulating K^+ transport during berry
557 maturation will likely help to stimulate advances in our knowledge of grapevine drought
558 stress adaptation, berry development, and the determinants of fruit acidity and quality.
559
560
561 Acknowledgements:
562 This work was supported by SweetKaliGrape ANR (ANR-33 14-CE20-0002-02). M.N.-C.
563 received a grant from the Marie Curie program (FP7-IEF, grant no. 272390), and M.A.
564 received a scholarship from the Conabex Commission of Madagascar.
565
566 Author contributions:
567 MN-C, MA and SZ performed electrophysiology experiments. TC and IG performed
568 cloning and q-PCR. TC and JLV performed *in situ* hybridization and histological
569 experiments. MB performed rooted cane cultures. BM, NP, MN-C and RG contributed
570 new reagents/analytic tools. IG conceived the project. analyzed the data and drafted the
571 manuscript.
572

References:

Ache P, Becker D, Deeken R, Dreyer I, Weber H, Fromm J, Hedrich R. 2001. VFK1, a Vicia faba K(+) channel involved in phloem unloading. *Plant J* **27**(6): 571-580.

Adir N, Zer H, Shochat S, Ohad I. 2003. Photoinhibition - a historical perspective. *Photosynth Res* **76**(1-3): 343-370.

Chatelet DS, Rost TL, Matthews MA, Shackel KA. 2008a. The peripheral xylem of grapevine (Vitis vinifera) berries. 2. Anatomy and development. *J Exp Bot* **59**(8): 1997-2007.

Chatelet DS, Rost TL, Shackel KA, Matthews MA. 2008b. The peripheral xylem of grapevine (Vitis vinifera). 1. Structural integrity in post-veraison berries. *J Exp Bot* **59**(8): 1987-1996.

Chérel I, Michard E, Platet N, Mouline K, Alcon C, Sentenac H, Thibaud JB. 2002. Physical and functional interaction of the Arabidopsis K(+) channel AKT2 and phosphatase AtPP2CA. *Plant Cell* **14**(5): 1133-1146.

Choat B, Gambetta GA, Shackel KA, Matthews MA. 2009. Vascular function in grape berries across development and its relevance to apparent hydraulic isolation. *Plant Physiol* **151**(3): 1677-1687.

Conde C, Silva P, Fontes N, Dias A, Tavares RM, Sousa MJ, Agasse A, Delrot S, Gerós H. 2007. Biochemical changes throughout grape berry development and fruit and wine quality. *Food* **1**: 1-22.

Cuéllar T, Azeem F, Andrianteranagna M, Pascaud F, Verdeil JL, Sentenac H, Zimmermann S, Gaillard I. 2013. Potassium transport in developing fleshy fruits: the grapevine inward K(+) channel VvK1.2 is activated by CIPK-CBL complexes and induced in ripening berry flesh cells. *Plant J* **73**(6): 1006-1018.

Cuéllar T, Pascaud F, Verdeil JL, Torregrosa L, Adam-Blondon AF, Thibaud JB, Sentenac H, Gaillard I. 2010. A grapevine Shaker inward K(+) channel activated by the calcineurin B-like calcium sensor 1-protein kinase CIPK23 network is expressed in grape berries under drought stress conditions. *Plant J* **61**(1): 58-69.

Davies C, Shin R, Liu W, Thomas MR, Schachtman DP. 2006. Transporters expressed during grape berry (Vitis vinifera L.) development are associated with an increase in berry size and berry potassium accumulation. *J Exp Bot* **57**(12): 3209-3216.

Deeken R, Geiger D, Fromm J, Koroleva O, Ache P, Langenfeld-Heyser R, Sauer N, May ST, Hedrich R. 2002. Loss of the AKT2/3 potassium channel affects sugar loading into the phloem of Arabidopsis. *Planta* **216**(2): 334-344.

Deeken R, Sanders C, Ache P, Hedrich R. 2000. Developmental and light-dependent regulation of a phloem-localised K+ channel of Arabidopsis thaliana. *Plant J* **23**(2): 285-290.

Dreyer I, Becker D, Bregante M, Gambale F, Lehnen M, Palme K, Hedrich R. 1998. Single mutations strongly alter the K+-selective pore of the K(in) channel KAT1. *FEBS Lett* **430**(3): 370-376.

Dreyer I, Gomez-Porras JL, Riedelsberger J. 2017. The potassium battery: a mobile energy source for transport processes in plant vascular tissues. *New Phytol.* **216**(4):1049-1053

Dreyer I, Michard E, Lacombe B, Thibaud JB. 2001. A plant Shaker-like K+ channel switches between two distinct gating modes resulting in either inward-rectifying or "leak" current. *FEBS Lett* **505**(2): 233-239.

Dreyer I, Uozumi N. 2011. Potassium channels in plant cells. *FEBS J* **278**(22): 4293-4303.

Duchêne E, Dumas V, Jaegli N, Merdinoglu D. 2014. Genetic variability of descriptors for grapevine berry acidity in Riesling, Gewürztraminer and their progeny. *Australian Journal of Grape and Wine Research* **20**(1): 91-99.

During H. 1988. CO2 assimilation and phosphorespiration of grapevine leaves: Responses to light and drought. *Vitis* **27**: 199-208.

Ehrhardt T, Zimmermann S, Muller-Rober B. 1997. Association of plant K+(in) channels is mediated by conserved C-termini and does not affect subunit assembly. *FEBS Lett* **409**(2): 166-170.

Esteban MA, Villanueva MJ, Lissarrague JR. 2001. Effect of irrigation on changes in the anthocyanin composition of the skin of cv. Tempranillo (Vitis vinifera L) grape berries during ripening. *Journal of the Science of Food and Agriculture.* **81**(4): 409–420.

Famiani F, Farinelli D, Frioni T, Palliotti A, Battistelli A, Moscatello S, Walker RP. 2016. Malate as substrate for catabolism and gluconeogenesis during ripening in the pericarp of different grape cultivars. *Biologia Plantarum* **60**(1): 155-162.

Findlay N, O, K. J., Nii N, Coombe BG. 1987. Solute accumulation by grape pericarp cells. IV. Perfusion of pericarp apoplast via the pedicel and evidence for xylem malfunction in ripening berries. *Journal of Experimental Botany* **38**: 668-679.

Gajdanowicz P, Michard E, Sandmann M, Rocha M, Correa LG, Ramirez-Aguilar SJ, Gomez-Porras JL, Gonzalez W, Thibaud JB, van Dongen JT, et al. 2011. Potassium (K+) gradients serve as a mobile energy source in plant vascular tissues. *Proc Natl Acad Sci U S A* **108**(2): 864-869.

Gorton HL. 1987a. Water Relations in Pulvini from Samanea saman: I. Intact Pulvini. *Plant Physiol* **83**(4): 945-950.

Gorton HL. 1987b. Water Relations in Pulvini from Samanea saman: II. Effects of Excision of Motor Tissues. *Plant Physiol* **83**(4): 951-955.

Hafke JB, Furch AC, Reitz MU, van Bel AJ. 2007. Functional sieve element protoplasts. *Plant Physiol* **145**(3): 703-711.

Hanana M, Cagnac O, Yamaguchi T, Hamdi S, Ghorbel A, Blumwald E. 2007. A grape berry (Vitis vinifera L.) cation/proton antiporter is associated with berry ripening. *Plant Cell Physiol* **48**(6): 804-811.

Held K, Pascaud F, Eckert C, Gajdanowicz P, Hashimoto K, Corratge-Faillie C, Offenborn JN, Lacombe B, Dreyer I, Thibaud JB, et al. 2011. Calcium-dependent modulation and plasma membrane targeting of the AKT2 potassium channel by the CBL4/CIPK6 calcium sensor/protein kinase complex. *Cell Res* **21**(7): 1116-1130.

Huang W, Yang SJ, Zhang SB, Zhang JL, Cao KF. 2012. Cyclic electron flow plays an important role in photoprotection for the resurrection plant Paraboea rufescens under drought stress. *Planta* **235**(4): 819-828.

Iandolino AB, Pearcy RW, Williams LE. 2013. Simulating three-dimensional grapevine canopies and modelling their light interception characteristics. *Australian Journal of Grape and Wine Research*: n/a-n/a.

Ivashikina N, Deeken R, Fischer S, Ache P, Hedrich R. 2005. AKT2/3 subunits render guard cell K+ channels Ca2+ sensitive. *J Gen Physiol* **125**(5): 483-492.

Jaillon O, Aury JM, Noel B, Policriti A, Clepet C, Casagrande A, Choisne N, Aubourg S, Vitulo N, Jubin C, et al. 2007. The grapevine genome sequence suggests ancestral hexaploidization in major angiosperm phyla. *Nature* **449**(7161): 463-467.

672 **Jones GV, White MA, Cooper OR, Storchmann K. 2005.** Climate Change and Global
673 Wine Quality. *Climatic Change* **73**(3): 319-343.
674 **Kanellis AK, Roubelakis - Angelakis KA 1993.** Grape. In: Seymour GB, Taylor JE,
675 Tucker GA eds. *Biochemistry of Fruit Ripening*. Dordrecht: Springer Netherlands,
676 189-234.
677 **Keller M 2015.** Partitioning of assimilates. In: Press A ed. *The Science of grapevines:*
678 *Anatomy and Physiology*. UK: Elsevier Inc., 145-187.
679 **Keller M, Smith JP, Bondada BR. 2006.** Ripening grape berries remain hydraulically
680 connected to the shoot. *J Exp Bot* **57**(11): 2577-2587.
681 **Kennedy JA., Matthews MA., Waterhouse AL**. 2002. Effect of maturity and vine water
682 status on grape skin and wine flavonoids. Am. J. Enol. Vitic. **53**: 268-274.
683 **Knipfer T, Fei J, Gambetta GA, McElrone AJ, Shackel KA, Matthews MA. 2015.**
684 Water Transport Properties of the Grape Pedicel during Fruit Development:
685 Insights into Xylem Anatomy and Function Using Microtomography. *Plant Physiol*
686 **168**(4): 1590-1602.
687 **Kodur S. 2011.** Effects of juice pH and potassium on juice and wine quality, and
688 regulation of potassium in grapevines through rootstocks (Vitis): a short review.
689 *Vitis* **50**(1): 1-6.
690 **Kuhn C, Grof CP. 2010.** Sucrose transporters of higher plants. *Curr Opin Plant Biol*
691 **13**(3): 288-298.
692 **Lacombe B, Pilot G, Michard E, Gaymard F, Sentenac H, Thibaud JB. 2000.** A
693 shaker-like K(+) channel with weak rectification is expressed in both source and
694 sink phloem tissues of Arabidopsis. *Plant Cell* **12**(6): 837-851.
695 **Langer K, Ache P, Geiger D, Stinzing A, Arend M, Wind C, Regan S, Fromm J,**
696 **Hedrich R. 2002.** Poplar potassium transporters capable of controlling K+
697 homeostasis and K+-dependent xylogenesis. *Plant J* **32**(6): 997-1009.
698 **Lecourieux F, Kappel C, Lecourieux D, Serrano A, Torres E, Arce-Johnson P, Delrot**
699 **S. 2014.** An update on sugar transport and signalling in grapevine. *J Exp Bot* **65**(3):
700 821-832.
701 **Lee Y, Satter RL. 1989.** Effects of white, blue, red light and darkness on pH of the
702 apoplast in the Samanea pulvinus. *Planta* **178**(1): 31-40.
703 **Lefoulon C, Boeglin M, Moreau B, Véry AA, Szponarski W, Dauzat M, Michard E,**
704 **Gaillard I, Chérel I. 2016.** The Arabidopsis AtPP2CA Protein Phosphatase
705 Inhibits the GORK K+ Efflux Channel and Exerts a Dominant Suppressive Effect
706 on Phosphomimetic-activating Mutations. *J Biol Chem* **291**(12): 6521-6533.
707 **Marten I, Hoth S, Deeken R, Ache P, Ketchum KA, Hoshi T, Hedrich R. 1999.** AKT3,
708 a phloem-localized K+ channel, is blocked by protons. *Proc Natl Acad Sci U S A*
709 **96**(13): 7581-7586.
710 **Michard E, Dreyer I, Lacombe B, Sentenac H, Thibaud JB. 2005a.** Inward rectification
711 of the AKT2 channel abolished by voltage-dependent phosphorylation. *Plant J*
712 **44**(5): 783-797.
713 **Michard E, Lacombe B, Poree F, Mueller-Roeber B, Sentenac H, Thibaud JB, Dreyer**
714 **I. 2005b.** A unique voltage sensor sensitizes the potassium channel AKT2 to
715 phosphoregulation. *J Gen Physiol* **126**(6): 605-617.
716 **Moran N. 2007.** Osmoregulation of leaf motor cells. *FEBS Lett* **581**(12): 2337-2347.
717 **Moshelion M, Becker D, Czempinski K, Mueller-Roeber B, Attali B, Hedrich R,**
718 **Moran N. 2002.** Diurnal and circadian regulation of putative potassium channels in
719 a leaf moving organ. *Plant Physiol* **128**(2): 634-642.

Mpelasoka BS, Schachtman DP, Treeby MT, Thomas MR. 2003. A review of potassium nutrition in grapevines with special emphasis on berry accumulation. *Australian Journal of Grape and Wine Research* **9**: 154-168.

Müller P, Li XP, Niyogi KK. 2001. Non-photochemical quenching. A response to excess light energy. *Plant Physiol* **125**(4): 1558-1566.

Nieves-Cordones M, Chavanieu A, Jeanguenin L, Alcon C, Szponarski W, Estaran S, Chérel I, Zimmermann S, Sentenac H, Gaillard I. 2014. Distinct amino acids in the C-linker domain of the Arabidopsis K+ channel KAT2 determine its subcellular localization and activity at the plasma membrane. *Plant Physiol* **164**(3): 1415-1429.

Pastenes C, Pimentel P, Lillo J. 2005. Leaf movements and photoinhibition in relation to water stress in field-grown beans. *J Exp Bot* **56**(411): 425-433.

Pastenes C, Porter V, Baginsky C, Horton P, Gonzalez J. 2004. Paraheliotropism can protect water-stressed bean (Phaseolus vulgaris L.) plants against photoinhibition. *J Plant Physiol* **161**(12): 1315-1323.

Philippar K, Buchsenschutz K, Abshagen M, Fuchs I, Geiger D, Lacombe B, Hedrich R. 2003. The K+ channel KZM1 mediates potassium uptake into the phloem and guard cells of the C4 grass Zea mays. *J Biol Chem* **278**(19): 16973-16981.

Philippar K, Fuchs I, Luthen H, Hoth S, Bauer CS, Haga K, Thiel G, Ljung K, Sandberg G, Bottger M, et al. 1999. Auxin-induced K+ channel expression represents an essential step in coleoptile growth and gravitropism. *Proc Natl Acad Sci U S A* **96**(21): 12186-12191.

Pratelli R, Lacombe B, Torregrosa L, Gaymard F, Romieu C, Thibaud JB, Sentenac H. 2002. A grapevine gene encoding a guard cell K(+) channel displays developmental regulation in the grapevine berry. *Plant Physiol* **128**(2): 564-577.

Rienth M, Torregrosa L, Sarah G, Ardisson M, Brillouet JM, Romieu C. 2016. Temperature desynchronizes sugar and organic acid metabolism in ripening grapevine fruits and remodels their transcriptome. *BMC Plant Biol* **16**(1): 164.

Ronzier E, Corratge-Faillie C, Sanchez F, Prado K, Briere C, Leonhardt N, Thibaud JB, Xiong TC. 2014. CPK13, a noncanonical Ca2+-dependent protein kinase, specifically inhibits KAT2 and KAT1 shaker K+ channels and reduces stomatal opening. *Plant Physiol* **166**(1): 314-326.

Sandmann M, Sklodowski K, Gajdanowicz P, Michard E, Rocha M, Gomez-Porras JL, Gonzalez W, Correa LG, Ramirez-Aguilar SJ, Cuin TA, et al. 2011. The K (+) battery-regulating Arabidopsis K (+) channel AKT2 is under the control of multiple post-translational steps. *Plant Signal Behav* **6**(4): 558-562.

Satter RL, Geballe GT, Applewhite PB, Galston AW. 1974. Potassium flux and leaf movement in Samanea saman. I. Rhythmic movement. *J Gen Physiol* **64**(4): 413-430.

Satter RL, Guggino SE, Lonergan TA, Galston AW. 1981. The effects of blue and far red light on rhythmic leaflet movements in samanea and albizzia. *Plant Physiol* **67**(5): 965-968.

Sharma T, Dreyer I, Riedelsberger J. 2013. The role of K(+) channels in uptake and redistribution of potassium in the model plant Arabidopsis thaliana. *Front Plant Sci* **4**: 224.

Sklodowski K, Riedelsberger J, Raddatz N, Riadi G, Caballero J, Chérel I, Schulze W, Graf A, Dreyer I. 2017. The receptor-like pseudokinase MRH1 interacts with the voltage-gated potassium channel AKT2. *Sci Rep* **7**: 44611.

Takahashi S, Badger MR. 2011. Photoprotection in plants: a new light on photosystem II damage. *Trends Plant Sci* **16**(1): 53-60.

Takahashi S, Bauwe H, Badger M. 2007. Impairment of the photorespiratory pathway accelerates photoinhibition of photosystem II by suppression of repair but not acceleration of damage processes in Arabidopsis. *Plant Physiol* **144**(1): 487-494.

Takahashi S, Whitney SM, Badger MR. 2009. Different thermal sensitivity of the repair of photodamaged photosynthetic machinery in cultured Symbiodinium species. *Proc Natl Acad Sci U S A* **106**(9): 3237-3242.

Uehlein N, Kaldenhoff R. 2008. Aquaporins and plant leaf movements. *Ann Bot* **101**(1): 1-4.

Velasco R, Zharkikh A, Troggio M, Cartwright DA, Cestaro A, Pruss D, Pindo M, Fitzgerald LM, Vezzulli S, Reid J, et al. 2007. A high quality draft consensus sequence of the genome of a heterozygous grapevine variety. *PLoS One* **2**(12): e1326.

Véry AA, Nieves-Cordones M, Daly M, Khan I, Fizames C, Sentenac H. 2014. Molecular biology of K+ transport across the plant cell membrane: what do we learn from comparison between plant species? *J Plant Physiol* **171**(9): 748-769.

Wada H, Shackel KA, Matthews MA. 2008. Fruit ripening in Vitis vinifera: apoplastic solute accumulation accounts for pre-veraison turgor loss in berries. *Planta* **227**(6): 1351-1361.

Yu L, Becker D, Levi H, Moshelion M, Hedrich R, Lotan I, Moran A, Pick U, Naveh L, Libal Y, et al. 2006. Phosphorylation of SPICK2, an AKT2 channel homologue from Samanea motor cells. *J Exp Bot* **57**(14): 3583-3594.

Yu L, Moshelion M, Moran N. 2001. Extracellular protons inhibit the activity of inward-rectifying potassium channels in the motor cells of Samanea saman pulvini. *Plant Physiol* **127**(3): 1310-1322.

Zhang XY, Wang XL, Wang XF, Xia GH, Pan QH, Fan RC, Wu FQ, Yu XC, Zhang DP. 2006. A shift of Phloem unloading from symplasmic to apoplasmic pathway is involved in developmental onset of ripening in grape berry. *Plant Physiol* **142**(1): 220-232.

Figure legends

Fig. 1: The grapevine Shaker K^+ channel family

(a) Phylogenetic relationships in the grapevine and *Arabidopsis thaliana* Shaker K^+ channel families. The Shaker family displays 5 groups in plants (Pilot *et al.*, 2003), named I through V. The *A. thaliana* Shaker family harboring voltage-dependent K^+ channels comprises 9 members: AKT1 (At2g26650), AKT5 (At4g32500) and SPIK (At2g25600) in group I; KAT1 (At5g46240) and KAT2 (At4g18290) in group II; AKT2 (At4g22200) in group III; AtKC1 (At4g32650) in group IV; and GORK (At5g37500) and SKOR (At3g02850) in group V. The grapevine Shaker family also comprises 9 members: VvK1.2 (NP_001268010.1; Cuéllar *et al.*, 2013), VvKT1.1 (CAZ64538; Cuellar *et al.*, 2010), VvK2.1 (NP_001268073; Pratelli *et al.*, 2002), VvK3.1 (XP_002268924 – this report), and 5 other members identified by *in silico* screening of the grapevine genome sequence as VvK4.1 (XP_003631831.1), VvK5.1 (NP_001268087), VvK5.2 (CBI16957.3), VvK5.3 (XP_002282398), and VvK5.4 (XP_002279184). The members belonging to group III are highlighted in grey.

(b) Representation of a Shaker alpha-subunit structure. A functional shaker channel is built of four alpha-subunits. Each subunit contains six transmembrane domains (S1-S6) and a pore domain (P) located between the S5 and S6 domains, which contains the hallmark TXGYGD/E motif imparting K^+ selectivity. The C terminus region contains various domains like the C-linker domain, the putative cyclic nucleotide-binding domain (CNBD), an ankyrin domain (Ank), and a domain rich in hydrophobic and acidic residues named K_{HA}.

Fig. 2: *VvK3.1* transcript levels in grapevine organs

Real-time quantitative PCR was performed on total RNA isolated from leaves or roots from rooted canes, or from leaves, stems, petioles, tendrils, flowers or berries from open field grapevines grown under standard irrigation.

(a) *VvK3.1* transcript levels of leaves, stems, petioles, tendrils and berries collected at fruit set.

(b) *VvK3.1* transcript levels of berries collected at different developmental stages (days after flowering). Stages corresponding to fruit set and veraison are indicated by arrows. The mean values and standard errors of two biological replicates are presented.

Fig. 3: ***In situ*** **localization of *VvK3.1* transcripts in flowers and berries at fruit set and ripening stages**

Longitudinal and equatorial sections were hybridized with *VvK3.1* RNA sense probe (left column: a1, a2, b1, c1, c2) and antisense probe (right columns). Sections hybridized with the sense probe (negative control) did not show any significant signal. A positive blue signal was observed in flowers (a), as well as in berries at fruit set (b) and at post-veraison (c), when the sections were hybridized with *VvK3.1* antisense probe.

(a) *Flowers*: signals were detected in the phloem, ovary and ovule. In the ovary, a blue color was observed in the epidermis bordering the ovarian locule. In the ovule, a strong signal was detected in the nucellus.

(b) *Berries at fruit set*: blue signals were observed in the endosperm and the phloem.

(c) *Berries during ripening*: an intense signal was detected in the vascular bundles, where the expression of VvK3.1 is restricted to phloem and perivascular cells.

CoS, channel of style; E, endosperm; End, endocarp; EOL, epidermis ovarian locule; Ep, epicarp; II, inner integument; IM, inner mesocarp; Mes, mesocarp; Nu, nucellus; O, ovule; OC, ovary cavity; OI, outer integument; OM, outer mesocarp; P, pericarp; Pe, perisperm; Ph, phloem; PVC, perivascular cells; S, style; SC, seed coat; St, stigmas; StB, stigma basis; VB, vascular bundles; Xy, xylem.

Fig. 4. Expression of *VvK3.1* in pulvinus structures located in the petiole

(a) Anatomical position of the pulvinus and cross sections. A vine branch was photographed before (a1) and after (a2) the onset of drought stress (brought on by stopping irrigation). Under drought stress, the petiole position dropped, becoming almost perpendicular to the stem. The positions of pulvinus structures (white arrows) are clearly visible, with one located toward the stem side and the other toward the leaf side. Cross sections of the petiole were observed by stereomicroscope (a3) or light microscope after histological staining (a4).

(b) Histological staining of petiole cross sections. Three-micrometer semi-thin sections were stained with naphthol blue-black and periodic acid-Schiff. Phloem elements are distinguishable by their dark purple cell walls stained by periodic acid-Schiff (b3). The pulvinus is composed of thin-walled parenchyma with intercellular spaces arranged around the vascular bundle (b2, b3).

(c) *In situ* hybridizations with the *VvK3.1* RNA sense probe (left column) and antisense probe (right column) are shown. A negative control was performed with *the VvK3.1* sense probe and no signal was observed (c1 and c2). When the cross sections were hybridized with *VvK3.1* antisense probe, intense signals (blue color) were detected in the phloem sap (c3, c4 and c6) and in the abaxial side of the pulvinus structure (c3, c5 and c6). No signal was observed on the adaxial side.

Ad.s, adaxial side; Ab.s, abaxial side; Ep, epiderm; ICL, innermost cell layer; OCL, outer cell layer; Ph, phloem; Pul, pulvinus; VB, vascular bundles; Xy, xylem.

Fig. 5. Regulation of VvK3.1 expression in response to drought stress

VvK3.1 transcript accumulation was analyzed by real-time quantitative PCR on total RNA. (a) Berries were collected from field-grown 4-year-old plants under controlled irrigation. Drought stress was applied by decreasing the level of irrigation for 15 days before berries were collected. At this point, the leaf water potential was then in the range of -0.7 to -0.6 MPa in drought stressed plants, compared with -0.2 MPa in control plants under standard irrigation. Absolute transcript levels of the control (white bars) or water-stressed berries (grey bars) were normalized using EF1-alpha transcript signals. (b) Leaves and (c) roots were collected from rooted canes. The plants were subjected to drought stress by stopping irrigation for 10 days. Data are expressed relative to *VvK3.1* transcript accumulation in plant material collected at t = 0. All data presented are the means (± SE) of two biological replicates.

Fig. 6. Characterization of the grapevine channel VvK3.1 in *Xenopus* oocytes

(a) Representative current traces in response to voltage-clamp pulses from +70 mV to -155 mV for VvK3.1 in 100 mM K^+ solution at pH 6.5. Note that instantaneous and time-activating inwardly rectifying currents are typically induced upon hyperpolarization.

(b) VvK3.1 currents are dependent on external potassium concentrations. Current-voltage curves of normalized VvK3.1 currents are compared at 100 (K100), 50 (K50) and 10 mM K^+ (K10) at pH 6.5 (n=6 ± SD). Steady-state currents at the end of voltage pulses as presented in (a) are plotted against the corresponding applied membrane potentials. Currents were normalized for each oocyte, setting the current value at -140 mV in K100 to -1. (c) Inhibition of VvK3.1 inward currents by 10 mM Cs^+. Voltage-dependent current inhibition of absolute mean currents is shown as a current-voltage curve (n=12 ± SD).

Fig. 7: The grapevine channel VvK3.1 is strongly regulated by pH

(a) VvK3.1 currents are regulated by external pH. Current-voltage curves are shown for normalized VvK3.1 currents in 100 mM K^+ at pH 5.5, 6.5 and 7.5 (n=15 ± SD). Currents were normalized for each oocyte, setting the current value at -140 mV in K100 pH 6.5 to -1. Note that the currents are reduced by external acidification.

(b) Proportion (*i.e.* percentage scale) of the time-dependent (grey) and instantaneous (black) currents as a function of external pH. (n=15 ± SD). Oocytes were injected with VvK3.1 cRNA and steady-state currents were recorded at -140 mV before analysis. Note that the proportion of instantaneous current is stronger at pH 5.5 than at pH 7.5.

Fig. 8: Activation of VvK3.1 by co-expression of grapevine CIPK/CBL partners in *Xenopus* oocytes

VvK3.1 currents are slightly stimulated by co-expression with VvCIPK02/05 and VvCBL04, and more significantly stimulated by co-expression with VvCIPK03 and VvCBL04.

(a) Representative current traces in response to voltage-clamp pulses from +70 mV to -140 mV for control oocytes injected with either water, VvCIPK03/VvCBL04, VvCIPK02/05/VvCBL04, VvK3.1, alone, or VvK3.1 with CIPK/CBL partners, in 100 mM K^+ solution at pH 6.5.

(b) Current-voltage curves of absolute VvK3.1 currents from the same oocyte batch on the same day are compared for expression of VvK3.1 alone or with the corresponding partners in 100 mM K^+ (K100) at pH 6.5 (n=10 mean ± SD). Steady-state currents at the end of the voltage pulses are plotted against the corresponding applied membrane potentials.

(c) Proportion of the time-dependent (grey) and instantaneous (black) currents calculated from steady-state current as recorded in (b) (n=16-17; mean ± SD). Note that there was no modification of the relative proportion of the instantaneous and time-dependent components of the VvK3.1 currents.

Supporting Information

Table S1: Primers used in this study.

Fig. S1**:** Localization of *VvK3.1* transcript in leaves by *in situ* hybridization.

Fig. S2: Localization of *VvK3.1* transcripts in roots by *in situ* hybridization.

Fig. S3**:** Reversal potential and Ba^{2+} inhibition**.**

Fig. S4**:** Phylogenetic relationships of CIPKs and CBLs in Arabidopsis and grapevine.

Fig. S5**:** Expression of VvK3.1 and VvK1.2 in perivascular cells as revealed by in situ hybridization

a)

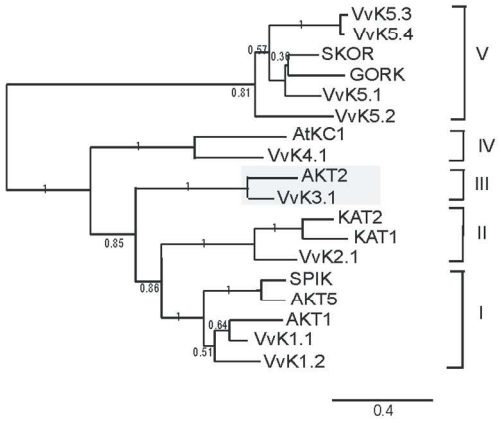

b)

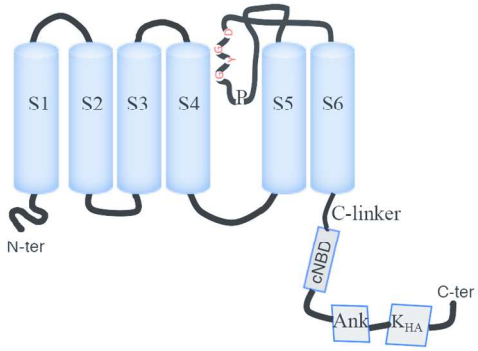

Figure 1

Fig.1: The grapevine Shaker K+ channel family

210x297mm (165 x 174 DPI)

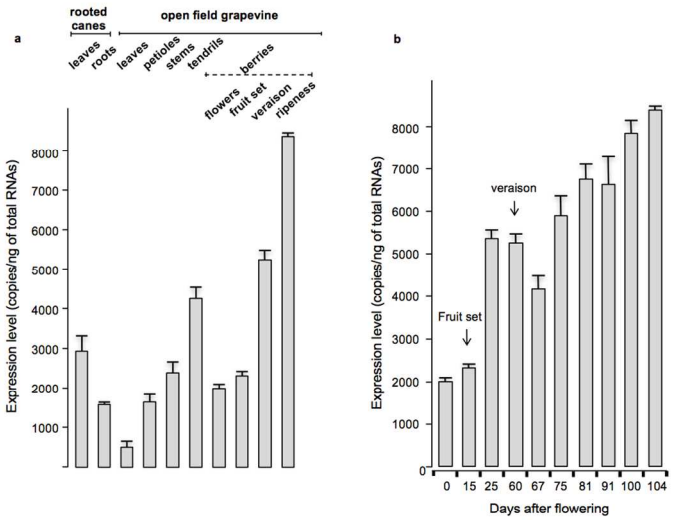

Figure 2

Fig. 2: VvK3.1 transcript levels in grapevine organs

209x297mm (150 x 150 DPI)

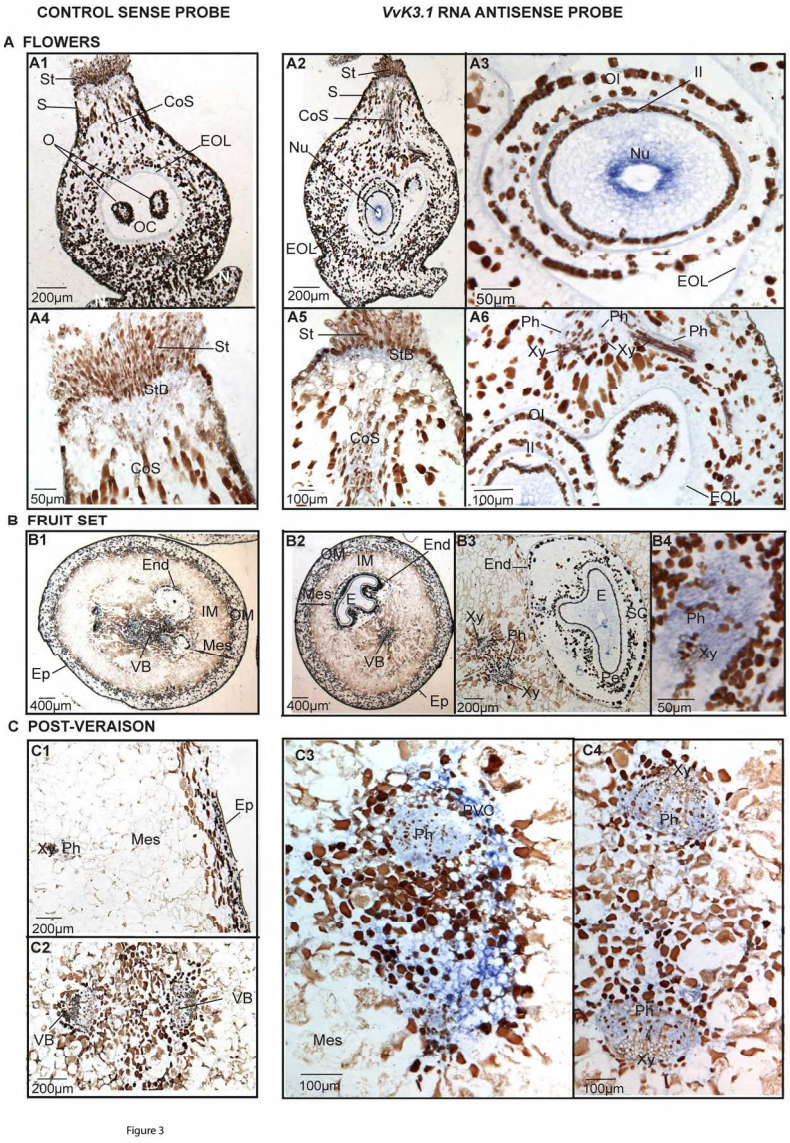

Figure 3

Fig. 3: In situ localization of VvK3.1 transcripts in flowers and berries at fruit set and ripening stages

300x450mm (150 x 150 DPI)

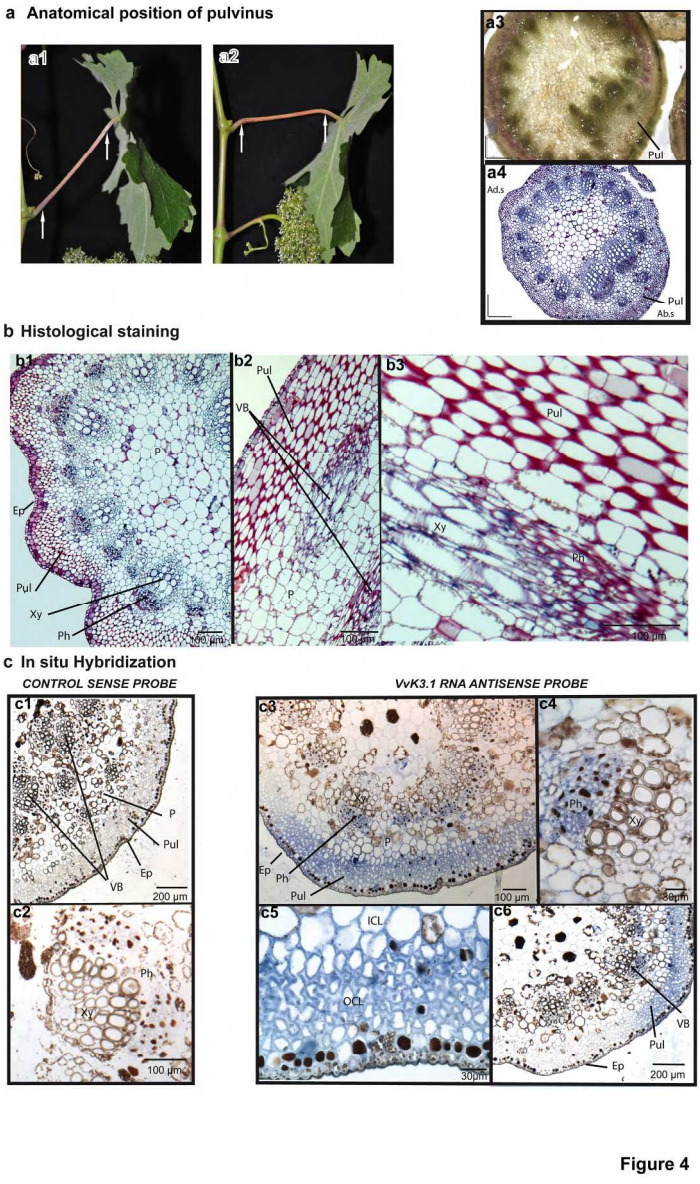

Figure 4

Fig. 4. Expression of VvK3.1 in pulvinus structures located in the petiole

306x522mm (150 x 150 DPI)

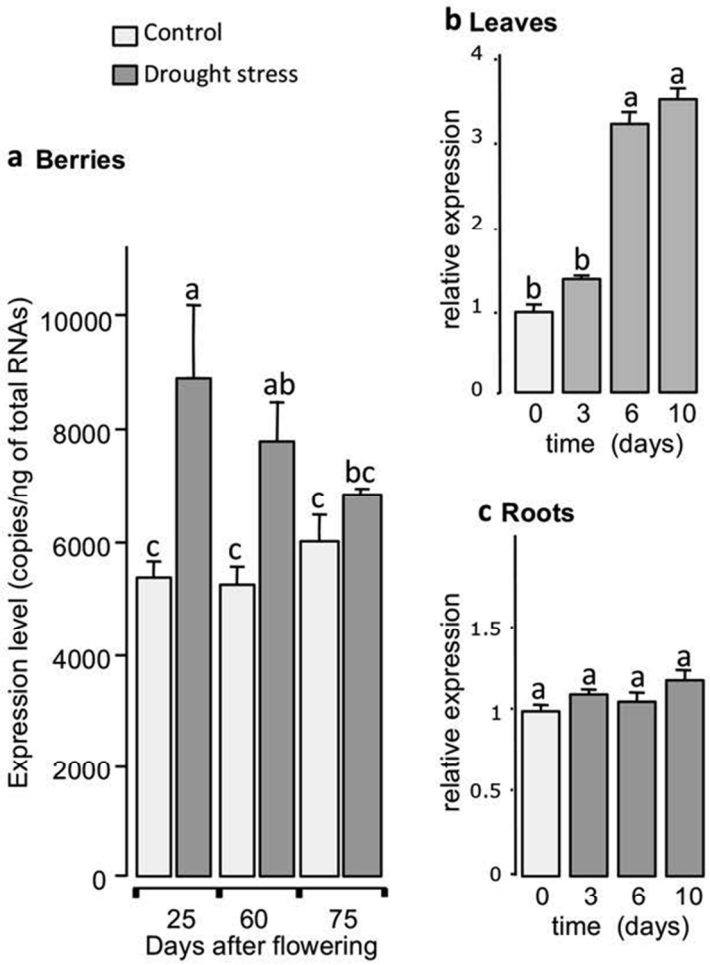

Figure 5

Fig. 5. Regulation of VvK3.1 expression in response to drought stress

160x263mm (100 x 100 DPI)

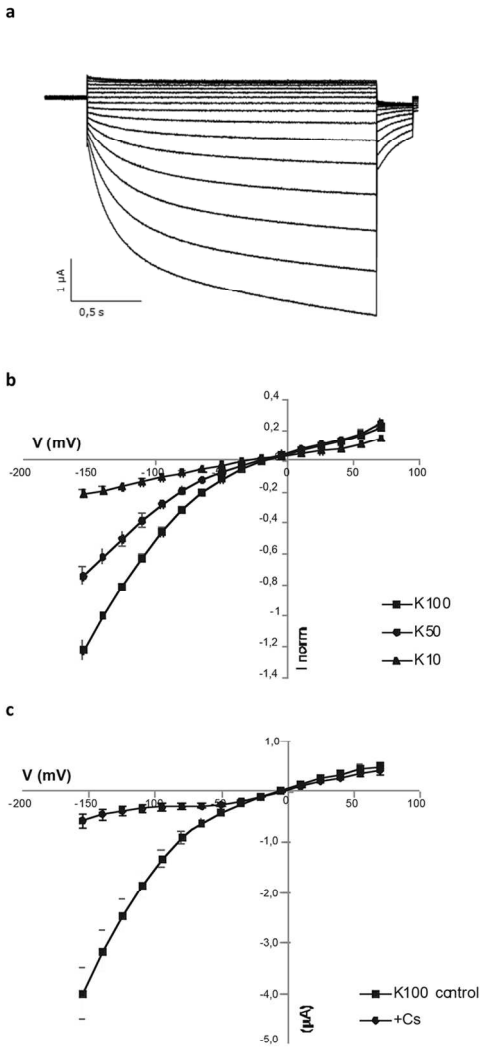

Figure 6

Fig. 6. Characterization of the grapevine channel VvK3.1 in Xenopus oocytes

295x546mm (300 x 300 DPI)

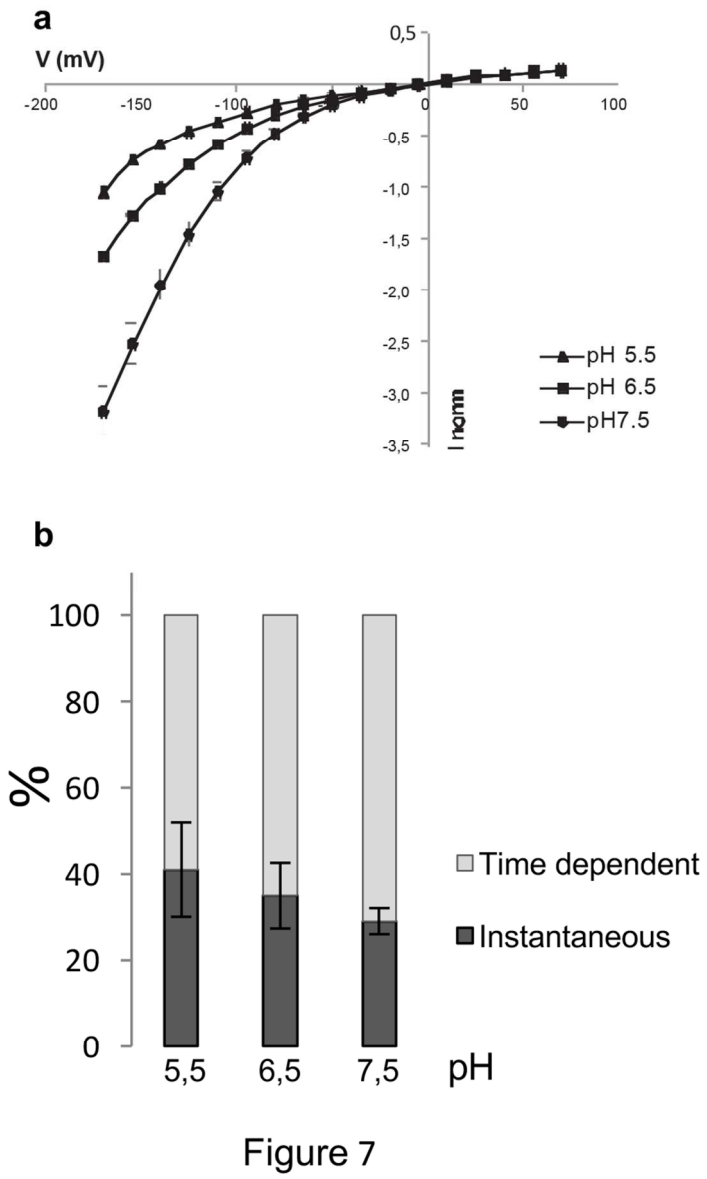

Figure 7

Fig. 7: The grapevine channel VvK3.1 is strongly regulated by pH

263x441mm (300 x 300 DPI)

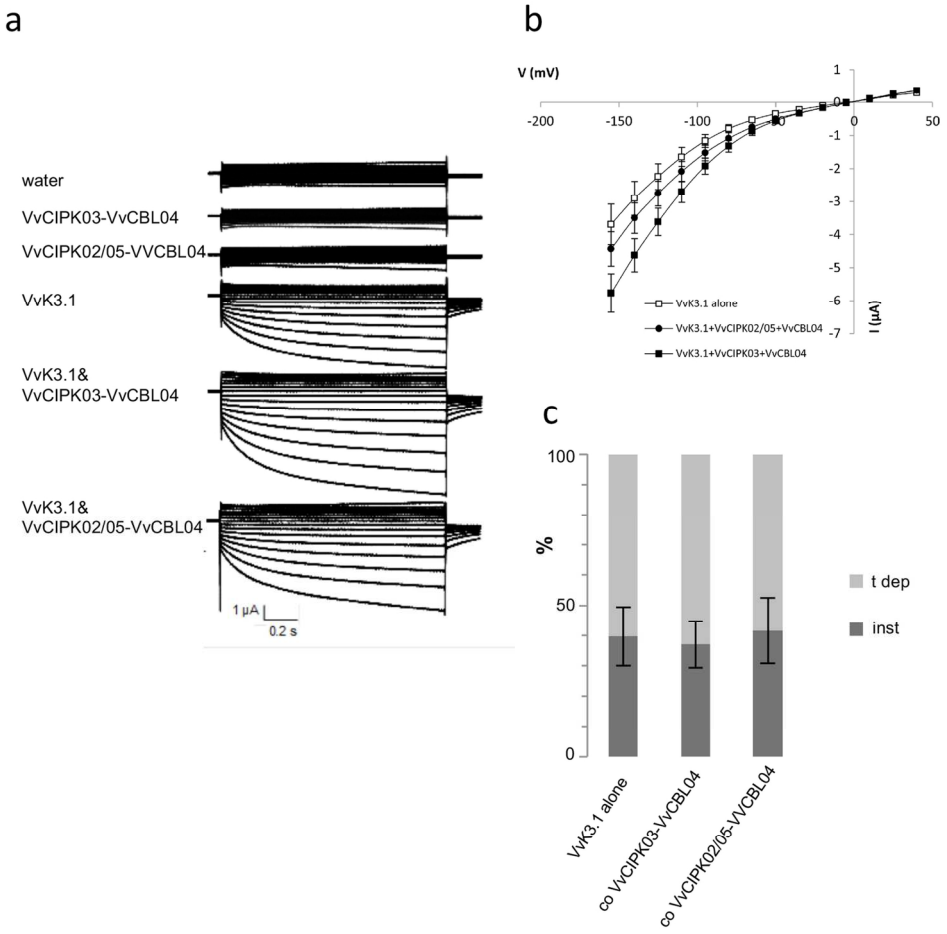

Figure 8

Fig. 8: Activation of VvK3.1 by co-expression of grapevine CIPK/CBL partners in Xenopus oocytes

170x182mm (300 x 300 DPI)